Journal of Materials Chemistry C

ROYAL SOCIETY OF CHEMISTRY

COMMUNICATION

View Article Online
View Journal | View Issue

Cite this: *J. Mater. Chem. C*, 2020, **8**, 10191

Received 5th May 2020,
Accepted 13th July 2020

DOI: 10.1039/d0tc02189j

rsc.li/materials-c

A bifacial colour-tunable system *via* combination of a cholesteric liquid crystal network and hydrogel†

Owies M. Wani, *[ab] Albertus P. H. J. Schenning [c] and Arri Priimagi *[a]

We present a colour tunable system obtained by combining a humidity-responsive cholesteric liquid crystal network and hydrogel coatings, in a diligently designed cell-geometry. The design enables sensitive colour tuning *via* temperature-induced changes in humidity inside the cell. Uniquely, the system exhibits a bifacial response, causing either a blue- or red-shift in the reflected color when heated from opposite sides.

Materials that can respond to external stimuli are at the forefront of contemporary materials research, owing to their enhanced versatility and tunable functionality as compared to conventional synthetic materials.[1–3] Such stimuli-responsive materials can, for instance, change their optical properties,[4,5] physical state,[6] macroscopic shape,[7,8] mechanical properties,[9] adhesion, or wettability,[10] when exposed to heat, light, humidity, pH, electric/magnetic fields, or a combination of these. Inspiration for such materials often times comes for the plethora of examples shown by naturally occurring responsive systems.[11]

Some of the intriguing cases are presented by species like the chameleon,[12] the blue damselfish[13] and some beetles,[14] which can change their body colour in response to changes in surroundings. Inspired by these phenomena, a significant amount of research activity has been dedicated towards developing artificial materials that are capable of reversibly changing their colour in response to external triggers.[5,15–18] The colour in these materials is mainly of a structural nature, *i.e.*, arising from the presence of photonic structures with periodically varying refractive indices.[14,16,19,20] Modulation of this periodicity using external triggers, through changes in either the thickness or refractive index of the structural features, can lead to a dynamic change in the structural colour.[18] Common material systems used for obtaining dynamic structural colour include inorganic solids,[5,21] hydrogels,[16] block copolymers[22,23] and liquid-crystalline polymers.[4,18] The dynamically changing colour renders these materials attractive for various applications, including energy-saving smart windows,[24] tunable lasers,[25] photonic paper,[5] colorimetric sensors,[26] and security coatings.[27]

Liquid crystals (LCs) are widely used in applications related to light control.[28] In their cholesteric state, LCs exhibit structural coloration due to the helical organization of molecules and the resultant periodic variation of the refractive index.[29] The periodicity of cholesteric LCs may undergo a stimuli-responsive change in the helical pitch, thereby leading to a change in the reflected colour.[4] Dynamically colour-changing low-molecular-weight and polymer-stabilized cholesteric LCs have been widely studied.[30–32] However, dynamic materials based on liquid crystal networks (LCNs) are becoming more and more attractive, due to their unique combination of anisotropic molecular order and elasticity of polymer networks.[33,34] In LCNs, changes in the molecular order can be triggered by, *e.g.*, heat, light, and humidity, which are inherently coupled to changes in the macroscopic dimensions of the material.

The cholesteric liquid crystal networks (ChLCNs) reported to date show a limited stimuli-induced strain. Therefore, devising a sensitive colour-changing ChLCN that responds to moderate energy input is challenging.[25,35–38] As the most notable recent advancement, Kragt *et al.* utilized a coating made by interpenetrating a siloxane-based LC polymer into an acrylate-based ChLCN. By varying the temperature, phase-separation and diffusion between the two interpenetrating polymers could be regulated, leading to tuning of the reflected colour.[37] As a second example, Brannum *et al.* used a cholesteric main-chain liquid crystal elastomer and demonstrated a temperature-controlled colour change across the whole visible spectrum. The colour

[a] *Smart Photonic Materials, Faculty of Engineering and Natural Sciences, Tampere University, P.O. Box 541, FI-33101 Tampere, Finland. E-mail: owies.wani@aalto.fi, arri.priimagi@tuni.fi*
[b] *Molecular Materials, Department of Applied Physics, Aalto University, P.O. Box 15100, FI-00076 Espoo, Finland*
[c] *Laboratory of Stimuli-Responsive Functional Materials and Devices (SFD), Department of Chemical Engineering and Chemistry, Eindhoven University of Technology (TU/e), P.O. Box 513, 5600 MB Eindhoven, The Netherlands*

† Electronic supplementary information (ESI) available. See DOI: 10.1039/d0tc02189j

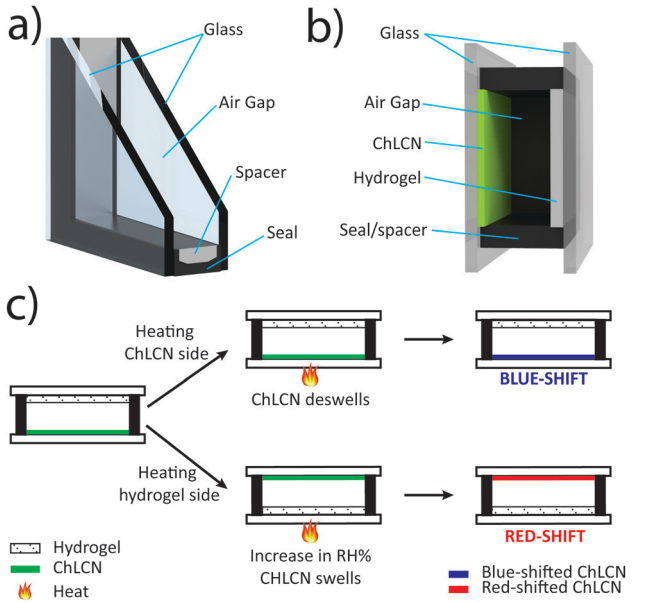

Fig. 1 Schematic representation of (a) a double-pane glass window and (b) the HumiCell. (c) The working principle of the HumiCell.

change was related to the thermomechanical deformation of the thickness of the cholesteric film.[38] These two systems are easily processable and technologically relevant, but the former suffers from slow kinetics, and the latter needs very high temperatures for the colour tuning. Stumpel *et al.*, on the other hand, used an interpenetrating network of an acrylate-based ChLCN and hydrogel to demonstrate a colour change in response to relative humidity (RH%) and pH.[39] Monali *et al.* prepared ChLCN coatings containing hydrogen-bonded carboxylic acid groups, which when treated with a basic solution were able to undergo fast colour tuning in response to humidity/temperature. While the humidity-responsive ChLCN coatings seem promising in terms of a large and fast response, due to the ever-changing atmospheric humidity, their integration in practical smart-window applications is challenging. Hence, there is a need for the development of novel material concepts for integrating humidity-responsive ChLCN coatings into potential applications.

In this work, we present a conceptual design that enables humidity-sensitive ChLCN coatings to respond indirectly to environmental temperature, irrespective of the prevailing atmospheric RH%. The design, which we coin as the HumiCell, also enables the system to show a bifacial nature, *i.e.*, an orthogonal response if stimulated on opposite sides. The HumiCell involves the synergistic use of ChLCN and hydrogel coatings, in a geometrical design resembling a double-pane window (Fig. 1a). The design is schematized in Fig. 1b and its working principle is illustrated in Fig. 1c. It consists of two glass plates separated by a gap of 1 mm. The gap is sealed on all sides to give rise to a small chamber. On the inner side, one of the glass plates is coated with a base-treated ChLCN layer and the other one is coated with a poly(acrylic acid) (PAA) hydrogel. The base-treated ChLCN layer is sensitive to both temperature and humidity, as reported previously.[40,41] Before sealing, a specific amount of water is loaded into the hydrogel, which in turn allows for controlling the relative humidity (RH%) inside the sealed chamber. The design enables unique bifacial characteristics, and the HumiCell behaves in an orthogonal manner when subjected to temperature variations from the opposite sides. Heating from the ChLCN side results in a blue-shift in the selective reflection, while heating from the hydrogel side causes a red-shift. The shift in reflection occurs at lower temperatures compared to previous reports of ChLCN-based systems[38] and the temperature range can be easily tuned by adjusting the amount of water absorbed into the hydrogel layer.

To realize the HumiCell, we used a humidity- and temperature-responsive ChLCN coating developed previously,[42] due to its fast response and large tunability. The ChLCN was fabricated from a mixture of commercially available LC mono- and diacrylates (including a chiral diacrylate giving rise to the cholesteric phase), a fraction of non-polymerizable LC (5CB), and a photoinitiator (Fig. 2a). The coating was photopolymerized in the cholesteric phase between the two glass plates, with alignment being achieved by shearing the glass plates prior to the photopolymerization. The PAA hydrogel was polymerized from the monomer mixture, also depicted in Fig. 2a. Further experimental details are given in the ESI.† One of the glass plates was silanized to ensure the firm attachment of the ChLCN coating/hydrogel to the substrate. After polymerization, once the other glass plate was removed, the ChLCN coating/hydrogel remained attached to the silanized glass plate. In the HumiCell, the average thickness of the ChLCN coating and the hydrogel layer is *ca.* 15 μm and 50 μm, respectively.

To make the ChLCN coating humidity-responsive, the pristine coating was first treated with THF to remove the 5CB. This improves the swelling capability of the network and enhances its stimuli-responsivity.[42] Then, the coating was treated with 1 M NaOH solution, which breaks the hydrogen bonds between the carboxylic acid end groups of the monomers and renders the polymer network hygroscopic. Fig. 2b depicts the changes in the transmission spectra of the ChLCN coating upon treatment with THF and basic solution and its inset shows the optical images of coatings at the corresponding stages of treatment. We studied the effect of an increase in RH% on the selective reflection of the ChLCN coating after the base treatment and observed that the increase in RH% caused a significant red-shift in the selective reflection, especially in the high-humidity range (Fig. 2c, red circles). This is due to swelling of the hygroscopic ChLCN, which increases the cholesteric pitch.[42] In a previous study, we discovered that the response of similar systems depends on the interplay between temperature and relative humidity.[40,41] Hence, we next studied the response of the coating to temperature at a fixed RH% (85%). As shown in Fig. 2c (blue triangles), heating causes a blue-shift in the reflection peak, which can be attributed to the release of water from the sample and a resultant decrease in the cholesteric pitch. Corresponding UV-vis transmission spectra of Fig. 2c are shown in Fig. S1 (ESI†).

After characterizing the ChLCN coating, we fabricated the HumiCell (fabrication details are given in the ESI†). PAA was

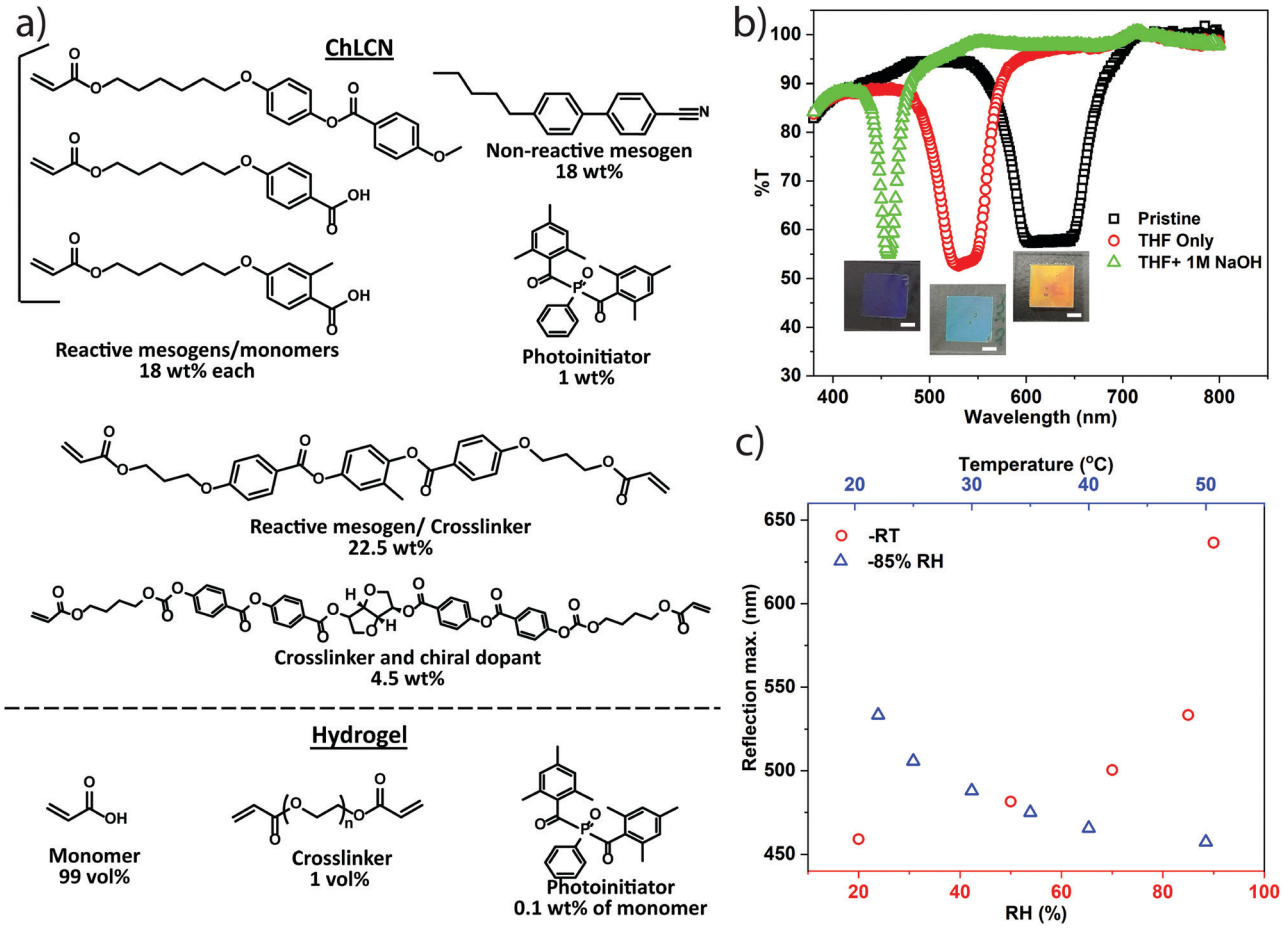

Fig. 2 (a) Chemical structures of molecules comprising the humidity- and temperature-responsive ChLCN and the hydrogel, (b) UV-vis transmission spectra of the ChLCN coating at various stages of treatment. Inset: Photographs of the ChLCN coatings at different stages of treatment, corresponding to the spectra above them. Scale bars: 5 mm. (c) Change in the reflection peak of the ChLCN in response to changes in RH% at RT (red circles) and changes in temperature at 85% RH (blue triangles).

chosen as the hydrogel, owing to its optical transparency and highly hydrophilic character.[43–45] Before sealing the hydrogel-coated glass to the ChLCN-coated glass, a specific amount of water was loaded into the hydrogel, and HumiCells with a range of different water contents were prepared. As the wt% water inside the hydrogel is increased, there is a red shift in the selective reflection peak of the cholesteric network (Fig. 3a) at room temperature, which indicates that there is a clear correlation between the amount of water inside the hydrogel and the relative humidity inside the sealed chamber. Each sample was characterized by heating the HumiCell from the hydrogel side, and the corresponding reflection maxima as a function of temperature are plotted in Fig. 3b. The related UV-vis transmission plots of Fig. 3a and b are shown in Fig. S2a and b, respectively (ESI†). Remarkably, heating the samples now causes a red shift in the reflection peak and the shift depends on the water content of the hydrogel. The higher the initial water content of the hydrogel, the more sensitive the HumiCell is to temperature, as attested by the increase in the slope of the curves shown in Fig. 3b with increasing water content. We attribute this phenomenon to a higher RH% in the chamber at a higher initial water content. At a higher temperature, more water is released from the hydrogel, leading to a higher RH% in the chamber and a red shift of the reflection peak. As the shift in reflection peak is most pronounced at high RH% (Fig. 2c), the sensitivity of the HumiCell can be tuned by the water content of the hydrogel. This observation provides a glimpse of the unique characteristics of the HumiCell system, in which both sensitivity and the temperature range can be chosen and tuned as desired. Note, however, that samples with very high water contents (>40 wt%) may exhibit condensation at high temperatures (see Video S1, ESI,† heating rate 5 °C min^{-1}).

For the following studies, we chose the sample with 36 wt% water content. Upon heating and cooling at 1 °C min^{-1} from the hydrogel side, we found the system to be reversible, exhibiting only small hysteresis. The peak shifts from the heating and cooling curves are shown in Fig. 4a and the corresponding optical images are given in Fig. 4b (see also Video S2, ESI,† for the heating/cooling rate of 5 °C min^{-1}). UV-vis transmission plots corresponding to Fig. 4a are shown in Fig. S3 (ESI†). We noticed that the edges of the cell are less sensitive than its central parts, which is most probably due to heat flow along the edge sealing, resulting in a decreased temperature gradient along the edges.

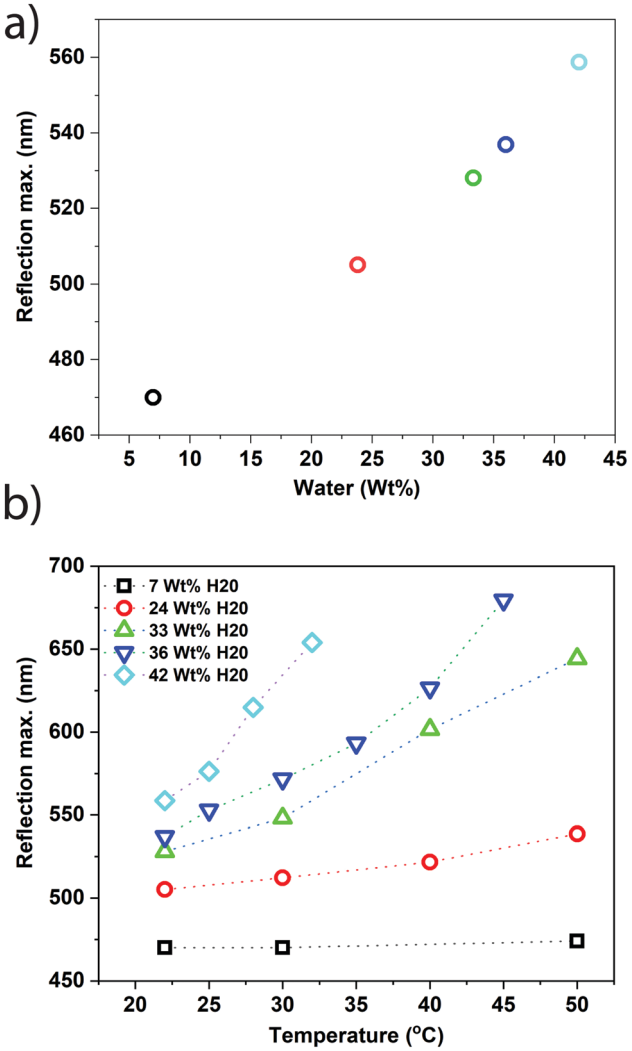

Fig. 3 (a) Reflection maxima of samples with different water contents at RT and (b) temperature-induced shift in the selective reflection of samples containing varying amounts of water, heated from the hydrogel side.

However, upon scaling up the device, which should be technically feasible, these edge effects would become insignificant.

To show the unique capability of the system to undergo red and blue shifts when heated from the hydrogel and ChLCN sides, we first recorded the transmission on a hot plate (at 40 °C) such that the sample was laying hydrogel side down. After that, the sample was flipped and heated from the ChLCN side, and the corresponding blue-shifted spectra were recorded (Fig. 4c). To test the kinetics of the HumiCell, we monitored the shift in reflection with time. The observed kinetics is plotted in Fig. 4d. The sample, placed on a hot plate hydrogel side down (40 °C) was flipped so that the ChLCN side comes in contact with the hot plate. At the same time, changes in the transmission spectra were monitored, and the sample underwent a blue-shift from 620 nm to 525 nm (Fig. 4d, blue circles). After that, the sample was again flipped to hydrogel side down, and the corresponding changes in transmission were recorded, revealing a red-shift of the reflection peak from 525 nm to 615 nm. The time constants for the blue and red shifts were estimated from exponential fittings to the curves shown in Fig. 4d and were found to be 0.4 and 2.3 min for the blue- and red-shift, respectively (see also Fig. S4, ESI†). The six times faster blue-shift (heating ChLCN side down) compared to the red-shift (heating from hydrogel side) can be explained by the different nature of the processes. Heating the ChLCN side causes desorption of water and thereby a decrease in the cholesteric pitch, which takes place relatively fast. However, heating from the hydrogel side involves two steps. First, water is released from the hydrogel, which increases the RH% of the cavity. The exact correlation between the temperature-induced water release and the RH% inside the chamber is a subject of future study.[46] Second, the increase in the RH% causes the humidity-sensitive ChLCN coating to swell, thereby leading to an increase in the cholesteric pitch.

The demonstrated concept provides a versatile means towards multi-responsive, high-sensitivity cholesteric reflectors, combining many aspects that are potentially relevant from a technological perspective. In addition to offering an indirect temperature response that is independent of the surrounding RH% (but being controlled by the humidity inside the sealed chamber), the system provides additional degrees of freedom. For instance, in smart window applications, the HumiCell can respond separately to changes in outside and inside temperatures, which is not possible with conventional ChLCN coating designs. This bifaciality is the unique feature of the HumiCell, which may also be utilized to make feedback-based self-regulating optical systems and tunable photonic components. The concept can also be extended to other types of hydrogels and ChLCN materials, optimized for an application of choice.

Conclusions

We have demonstrated a cholesteric liquid-crystal network (ChLCN)-based system – the HumiCell – which shows high temperature sensitivity, fast kinetics and versatile tuning of the colour-changing behaviour. The system enables a humidity sensitive reflective coating to respond to temperature changes irrespective of the external RH% and is capable of a reversible 100 nm shift in reflection by merely a 12 °C temperature change within a time scale of a few minutes. The most intriguing feature of the HumiCell, due to the unique geometry combining ChLCN and hydrogel coatings, is its bifacial response, leading to a red-shift in reflection when heated from the hydrogel side and a blue-shift when heated from the ChLCN side. We believe that this demonstration will open new possibilities in the design of self-regulating smart windows, tunable lasers, aesthetics, *etc.* Due to the design similarities with double-pane windows, the concept may offer easy integration with already established technologies.

Conflicts of interest

There are no conflicts to declare.

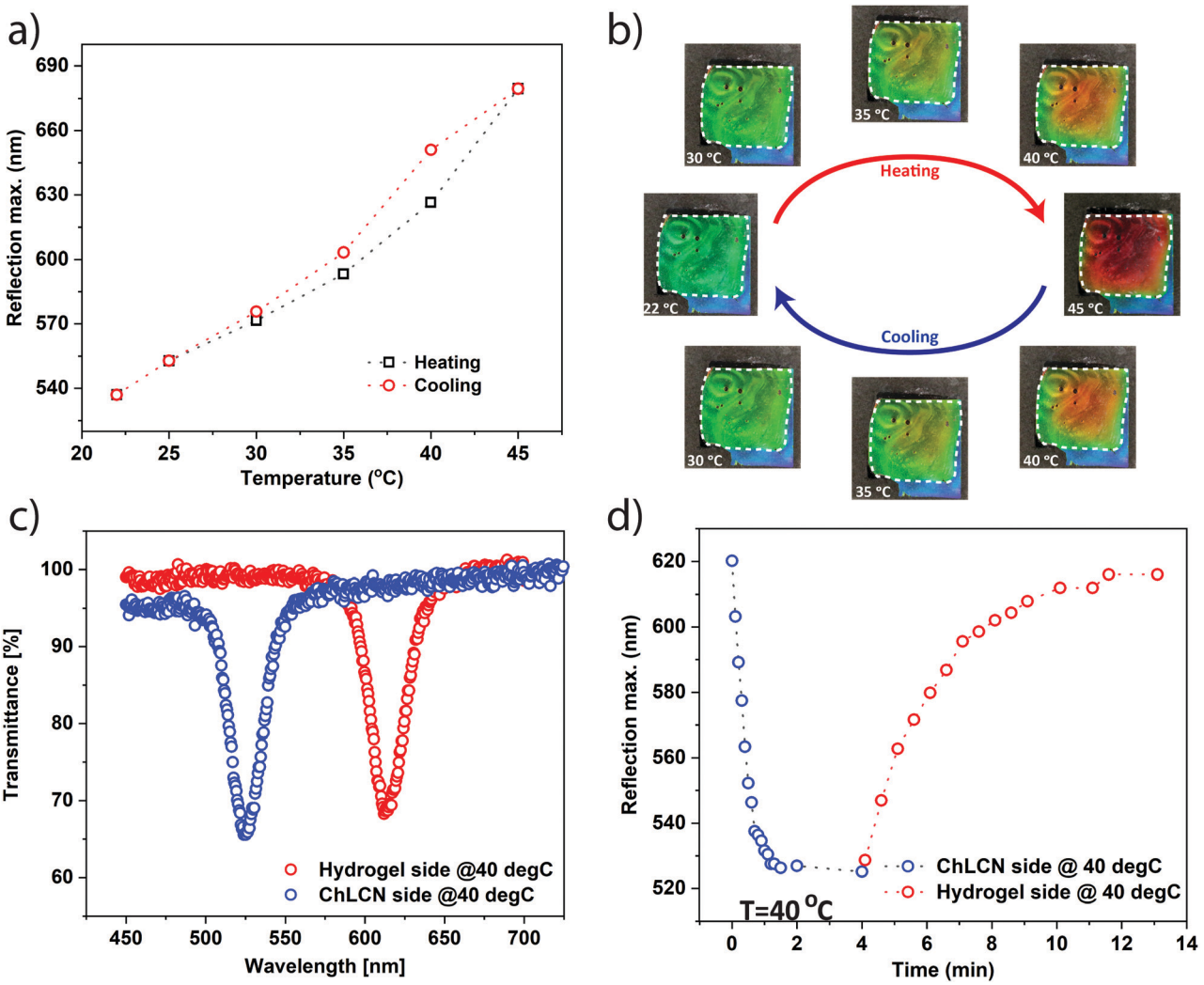

Fig. 4 (a) Shift in the reflection peak by heating and cooling from hydrogel side (probed along the centre of the sample), along with (b) the corresponding optical images. The blue colour is the part of the ChLCN coating covered by the sealing tape, hence it is inactive. The active area is marked with a white dashed line. (c) Red and blue shift in reflection peak upon heating on the hydrogel side (red circles) and the ChLCN side (blue circles), respectively. (d) Monitoring shift in reflection peak with time, upon heating the ChLCN side (blue circles) and the hydrogel side (red circles).

Acknowledgements

The work is part of the Academy of Finland Flagship Programme, Photonics Research and Innovation (PREIN), decision number 320165. The work is supported by the European Research Council (ERC Starting Grant Project PHOTOTUNE, Agreement No. 679646).

References

1 M. A. C. Stuart, W. T. S. Huck, J. Genzer, M. Müller, C. Ober, M. Stamm, G. B. Sukhorukov, I. Szleifer, V. V. Tsukruk, M. Urban, F. Winnik, S. Zauscher, I. Luzinov and S. Minko, *Nat. Mater.*, 2010, **9**, 101–113.
2 C. De Las Heras Alarcón, S. Pennadam and C. Alexander, *Chem. Soc. Rev.*, 2005, **34**, 276–285.
3 J. Shi, N. M. Alves and J. F. Mano, *Adv. Funct. Mater.*, 2007, **17**, 3312–3318.
4 T. J. White, M. E. McConney and T. J. Bunning, *J. Mater. Chem.*, 2010, **20**, 9832–9847.
5 J. Ge and Y. Yin, *Angew. Chem., Int. Ed.*, 2011, **50**, 1492–1522.
6 X. Yan, F. Wang, B. Zheng and F. Huang, *Chem. Soc. Rev.*, 2012, **41**, 6042–6065.
7 J. Leng, X. Lan, Y. Liu and S. Du, *Prog. Mater. Sci.*, 2011, **56**, 1077–1135.
8 S. J. Jeon, A. W. Hauser and R. C. Hayward, *Acc. Chem. Res.*, 2017, **50**, 161–169.
9 L. Montero De Espinosa, W. Meesorn, D. Moatsou and C. Weder, *Chem. Rev.*, 2017, **117**, 12851–12892.
10 F. Xia and L. Jiang, *Adv. Mater.*, 2008, **20**, 2842–2858.
11 J. S. Mohammed and W. L. Murphy, *Adv. Mater.*, 2009, **21**, 2361–2374.
12 J. Teyssier, S. V. Saenko, D. Van Der Marel and M. C. Milinkovitch, *Nat. Commun.*, 2015, **6**, 1–7.
13 D. Gur, B. A. Palmer, S. Weiner and L. Addadi, *Adv. Funct. Mater.*, 2017, **27**, 1603514.

14 J. Sun, B. Bhushan and J. Tong, *RSC Adv.*, 2013, **3**, 14862–14889.
15 Y. Zhao, Z. Xie, H. Gu, C. Zhu and Z. Gu, *Chem. Soc. Rev.*, 2012, **41**, 3297–3317.
16 C. I. Aguirre, E. Reguera and A. Stein, *Adv. Funct. Mater.*, 2010, **20**, 2565–2578.
17 E. Tian, J. Wang, Y. Zheng, Y. Song, L. Jiang and D. Zhu, *J. Mater. Chem.*, 2008, **18**, 1116–1122.
18 E. P. A. van Heeswijk, A. J. J. Kragt, N. Grossiord and A. P. H. J. Schenning, *Chem. Commun.*, 2019, **55**, 2880–2891.
19 B. Yang, F. Cai, S. Huang and H. Yu, *Angew. Chem., Int. Ed.*, 2020, **59**, 4035–4042.
20 M. Quan, B. Yang, J. Wang, H. Yu and X. Cao, *ACS Appl. Mater. Interfaces*, 2018, **10**, 4243–4249.
21 M. R. Jorgensen, B. P. Yonkee and M. H. Bartl, *Scr. Mater.*, 2011, **65**, 954–957.
22 S. Valkama, H. Kosonen, J. Ruokolainen, T. Haatainen, M. Torkkeli, R. Serimaa, G. Ten Brinke and O. Ikkala, *Nat. Mater.*, 2004, **3**, 872–876.
23 E. Kim, S. Y. Kim, G. Jo, S. Kim and M. J. Park, *ACS Appl. Mater. Interfaces*, 2012, **4**, 5179–5187.
24 A. Azens and C. Granqvist, *J. Solid State Electrochem.*, 2003, **7**, 64–68.
25 A. Varanytsia, H. Nagai, K. Urayama and P. Palffy-Muhoray, *Sci. Rep.*, 2015, **5**, 17739.
26 I. B. Burgess, M. Lončar and J. Aizenberg, *J. Mater. Chem. C*, 2013, **1**, 6075–6086.
27 B. Baloukas and L. Martinu, *Appl. Opt.*, 2008, **47**, 1585–1593.
28 D. Demus, *Cryst. Res. Technol.*, 1992, **27**, 40.
29 T. J. Bunning, *Liq. Cryst. Today*, 2014, **23**, 23–24.
30 R. Parker, *US Pat.*, US3861213, 1975.
31 D. K. Yang, *IEEE/OSA J. Disp. Technol.*, 2006, **2**, 32–37.
32 M. Mitov, *Adv. Mater.*, 2012, **24**, 6260–6276.
33 T. J. White and D. J. Broer, *Nat. Mater.*, 2015, **14**, 1087–1098.
34 C. Ohm, M. Brehmer and R. Zentel, *Adv. Mater.*, 2010, **22**, 3366–3387.
35 S. T. Kim and H. Finkelmann, *Macromol. Rapid Commun.*, 2001, **22**, 429–433.
36 J. Lub, D. J. Broer, R. A. M. Hikmet and K. G. J. Nierop, *Liq. Cryst.*, 1995, **18**, 319–326.
37 A. J. J. Kragt, N. C. M. Zuurbier, D. J. Broer and A. P. H. J. Schenning, *ACS Appl. Mater. Interfaces*, 2019, **11**, 28172–28179.
38 M. T. Brannum, A. M. Steele, M. C. Venetos, L. S. T. J. Korley, G. E. Wnek and T. J. White, *Adv. Opt. Mater.*, 2019, **7**, 1–7.
39 J. E. Stumpel, E. R. Gil, A. B. Spoelstra, C. W. M. Bastiaansen, D. J. Broer and A. P. H. J. Schenning, *Adv. Funct. Mater.*, 2015, **25**, 3314–3320.
40 O. M. Wani, R. Verpaalen, H. Zeng, A. Priimagi and A. P. H. J. Schenning, *Adv. Mater.*, 2019, **31**, 1805985.
41 E. P. A. Van Heeswijk, J. J. H. Kloos, N. Grossiord and A. P. H. J. Schenning, *J. Mater. Chem. A*, 2019, **7**, 6113–6119.
42 M. Moirangthem and A. P. H. J. H. J. Schenning, *ACS Appl. Mater. Interfaces*, 2018, **10**, 4168–4172.
43 A. A. Borisevich, A. E. Chalyh, G. S. Kulagina and V. K. Gerasimov, *Prot. Met. Phys. Chem. Surf.*, 2009, **45**, 675–678.
44 J. Wang, S. Ren and M. Guo, *Procedia Eng.*, 2012, **27**, 423–430.
45 J. E. Elliott, M. MacDonald, J. Nie and C. N. Bowman, *Polymer*, 2004, **45**, 1503–1510.
46 M. Poutanen, Z. Ahmed, L. Rautkari, O. Ikkala and A. Priimagi, *ACS Macro Lett.*, 2018, **7**, 381–386.